OPEN

Fabrication and Electrical Properties of Stacked Graphene Monolayers

Jing-Jing Chen[1], Jie Meng[1], Da-Peng Yu[1,2] & Zhi-Min Liao[1,2]

[1]State Key Laboratory for Mesoscopic Physics, Department of Physics, Peking University, Beijing 100871, P.R. China, [2]Collaborative Innovation Center of Quantum Matter, Beijing, China.

We develop a simple method to fabricate the two-stacked graphene monolayers and investigate the electronic transport in such a system. The independence of the two graphene monolayers gives rise to the asymmetric resistance-gate voltage curves and an eight-fold degeneracy of Landau level. The position of the maximum resistance of the transfer curves shifts towards higher gate voltage with increasing magnetic field, which is attributed to the magnetic field induced interlayer decoupling of the stacked graphene monolayers.

Rapid advances in the fabrication and transfer techniques of graphene have now provided researchers with a variety of structures that have remarkably distinct electronic properties[1–6]. The two graphene layers with inter-layer dielectric such as boron-nitride and Al_2O_3, were achieved experimentally to observe the Coulomb drag effect[7–9]. Theoretical studies have predicted the condensation of electron-hole pairs in such a quantum-bilayer system[10,11]. Graphene heterostructures with atomically thin boron-nitride or molybdenum disulfide as a vertical transport barrier, exhibit remarkably high conductance switching ratios of ~50 and ~10^4 at room temperature, respectively[3]. In these devices, an insulating spacer is necessary to separate the graphene monolayers. The structural diversity of the two-stacked graphene monolayers, that is the layers are stacked on top of each other, nourishes hopes for future graphene based electronics[12–15]. The two-stacked graphene monolayers can be synthesized by chemical vapor deposition (CVD)[16], identifying exfoliated fragments with folds[17] or using a polymethyl methacrylate (PMMA)-transfer technique to stack two graphene monolayers[18]. Sequences of quantum Hall plateaus were formed for two independent graphene monolayers with electronic screening taken into account[4,8,12]. Independent contributions to the magnetoresistance (MR) from the Landau level spectrum of each layer were demonstrated in the two-stacked graphene monolayers[17–19]. However, for a total filling factor of zero, the inter-layer interaction leads to an insulating state which cannot be explained by completely independent monolayer graphene sheets in parallel conductance[18]. The coupling and decoupling of the two-stacked graphene monolayers still need further experimental studies.

Here, we develop a new method of mass production of two-stacked graphene monolayers with a clean interface. We perform Raman and electronic transport measurements on our two-stacked graphene monolayers. The Raman spectrum similar to that of a monolayer graphene shows that the two graphene monolayers remain independent. We observe asymmetric transfer curves in the field effect transistors based on the two-stacked graphene monolayers. The position of the maximum resistance of the transfer curves shifts towards higher gate voltage with increasing magnetic field because of the magnetic field induced decoupling of the two graphene monolayers. The system exhibits large positive magnetoresistance for the discrepancy of the carrier mobilities in the two graphene monolayers. The two-stacked graphene monolayers show electronic properties quite different from single-crystal monolayer and bilayer systems.

Results

Monolayer graphene was grown using CVD method on Cu foils[20]. The monolayer graphene has a Hall mobility ~3900 cm^{-2}/V•s. Figure 1(a) displays the back-gate voltage (V_g) dependence of the resistivity and Hall conductivity of a typical monolayer graphene device at 1.8 K and 14 T. The Hall plateaus at ±2, 6, 10… are well formed, which show good quality of the monolayer graphene. The MR curves at two back-gate voltages of 0 V and 7 V at 1.8 K are shown in Fig. 1(b). The MR shows clear Shubnikov-de Haas (SdH) oscillations.

The as-grown monolayer graphene was used to fabricate the two-stacked graphene monolayers based on our transfer techniques[20]. A new method was developed to fabricate the stacked graphene monolayers without any PMMA between the graphene layers. Details of the fabrication of the stacked graphene monolayers are shown in Fig. 2(a). First, a PMMA thin layer was spin-coated on a monolayer graphene surface grown on copper foil. The
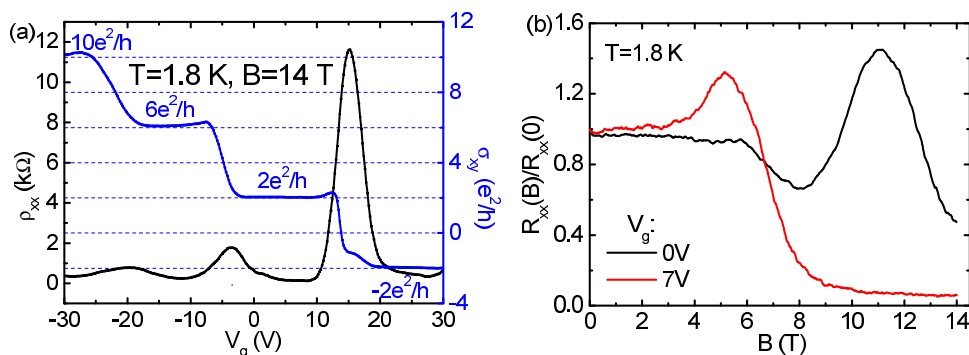
Figure 1 | Low temperature electronic transport in a monolayer graphene grown by CVD. (a) The longitudinal resistivity ρ_{xx} and Hall conductivity σ_{xy} as a function of back gate voltage V_g. (b) The magnetoresistance described as $R_{xx}(B)/R_{xx}(0)$ as a function of magnetic field at $V_g = 0$ V, 7 V.

Cu foil was then dissolved by $FeCl_3$ saturated solution for 30 min. The graphene/PMMA film was washed three times by 60°C deionized (DI) water. Another monolayer graphene on copper foil was used to fish out the graphene/PMMA film from deionized water. Because of the face-to-face superposition of clean graphene surfaces, there is no any PMMA between the graphene layers. The two-stacked graphene monolayers/PMMA film was then patterned into microstamps via electron beam lithography (EBL) and O_2 plasma etching. After the Cu foil was dissolved and the film was rinsed, the two-stacked graphene monolayers/PMMA microstamps can be transferred onto arbitrary substrate. The optical image of one typical two-stacked graphene monolayers microstamp transferred on SiO_2/Si substrate is shown in Fig. 2(b). Figure 2(c) shows the Raman spectrum of the two-stacked graphene monolayers, which is nearly the same as the monolayer graphene. It means that there is no lattice coupling between graphene layers. A weak D band implies a bit of lattice defects in graphene.

As shown in Fig. 3(a), the two-stacked graphene monolayers were patterned into Hall bar configuration with a length of 6 μm and a width of 2 μm. The electrodes were formed by 5 nm/75 nm Ti/Au thin film. The back-gate voltage dependence of the longitudinal resistance (R_{xx}) at 1.9 K is displayed in Fig. 3(b). The maximum of the resistance locates at $V_g = 37.5$ V and the transfer curve exhibits asymmetric behavior with respect to 37.5 V. In particular, the two graphene monolayers may have different Dirac points because the bottom graphene contacts with the SiO_2 layer while the top graphene is exposed to the atmosphere. Besides, with screening taken into account the carrier density in top graphene will be less sensitive to gate voltage than that of the bottom graphene. The $R_{xx} - V_g$ curve can be explained by the parallel conduction of the two independent monolayer graphene sheets. The total conductivity can be expressed as $\sigma = \sigma_T + \sigma_B$, where the conductivities of top and bottom graphene are $\sigma_T = n_T e \mu_T$ and $\sigma_B = n_B e \mu_B$, respectively. μ_T and μ_B are the carrier mobilities in the top/bottom graphene sheets, respectively.
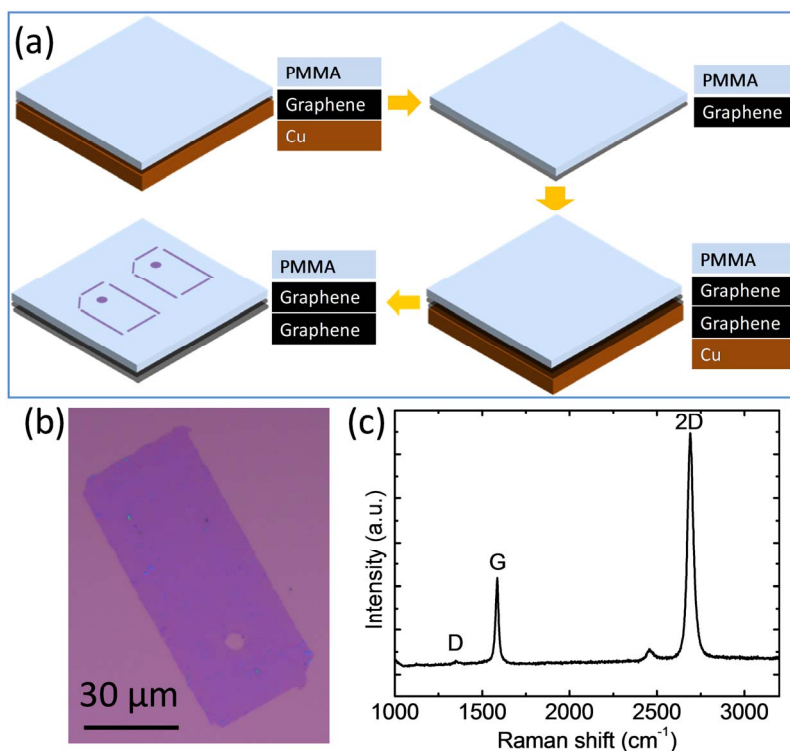

Figure 2 | Fabrication and characterization of two-stacked graphene monolayers. (a) Details of the fabrication process of the two-stacked graphene monolayers/PMMA microstamps. (b) Optical image of typical two-stacked graphene monolayers transferred on SiO_2/Si substrate. (c) Raman spectrum of the two-stacked graphene monolayers.
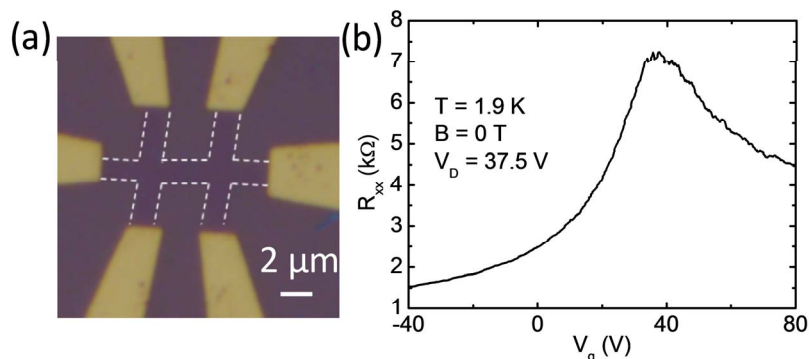
Figure 3 | Devices based on two-stacked graphene monolayers. (a) Optical image of a two-stacked graphene monolayers patterned into Hall bar configuration. (b) The longitudinal resistance R_{xx} as a function of back gate voltage V_g at 1.9 K.

$n_T = C_T|V_g - V_{D,T}|$ and $n_B = C_B|V_g - V_{D,B}|$ are carrier densities in the two graphene sheets, where $V_{D,T}$, $V_{D,B}$ are the Dirac neutral points, C_T and C_B are the capacitances between the top/bottom graphene sheets and the gate electrode. Then the total conductivity $\sigma = C_T e\mu_T|V_g - V_{D,T}| + C_B e\mu_B|V_g - V_{D,B}|$, where e is the charge element. When V_g is between $V_{D,T}$ and $V_{D,B}$, the slope for $\sigma - V_g$ curve is $|C_B e\mu_B - C_T e\mu_T|$ and is much smaller than $C_B e\mu_B + C_T e\mu_T$. So the resistance is less sensitive to the back-gate voltage between $V_{D,T}$ and $V_{D,B}$. Figure 3(b) shows that the resistance is less sensitive to the back-gate voltage near the $V_g = 37.5$ V.

We investigated the magnetotransport at low temperatures, as shown in Fig. 4. Unlike the pristine monolayer graphene (see Fig. 1(b)), the two-stacked graphene monolayers exhibit large positive MR background superimposed with SdH oscillations. This is probably due to the discrepancy of the carrier mobilities in the two graphene monolayers[21]. In particular, the electrons deflect from the current direction without the Hall voltages balancing the Lorentz force in the two graphene monolayers simultaneously. We estimated the average Hall mobility at $V_g = 0$ V to be 2500 $cm^2V^{-1}s^{-1}$. It is worth noting that the Hall resistivity increased with increasing the

magnetic field and then decreasing above 6 T for a back-gate voltage of 40 V. This is also observed in graphene with electron-hole coexistence in disordered graphene[22]. In our system, electrons exist in the bottom graphene and holes in the top graphene when applied a back-gate voltage of 40 V.

Discussion

Figures 4(c) and 4(d) display the gate voltage dependence of the resistance at various magnetic fields. As shown in Fig. 4(c), the SdH oscillations are not as clear as that in monolayer graphene (see Fig. 1(a)). At 14 T, the interspace of the two neighboring oscillation valleys near the Dirac point is $\Delta V_g = 40$ V, corresponding to the difference of the carrier density $\Delta n = 2.7 \times 10^{12}$ cm^{-2} due to the gate efficiency of the SiO_2 dialectical layer. The number of carrier states of each Landau level is $\Delta n = geB/h$, where g is the degeneration factor of the Landau level, h is the Planck's constant. Therefore, we can calculate that g equals 8 for the two-stacked graphene monolayers. At 300 K, we also clearly observed that the position of the resistance maxima shifts toward higher gate voltage as increasing the magnetic field (Fig. 4(d)), which indicates that the tunability of
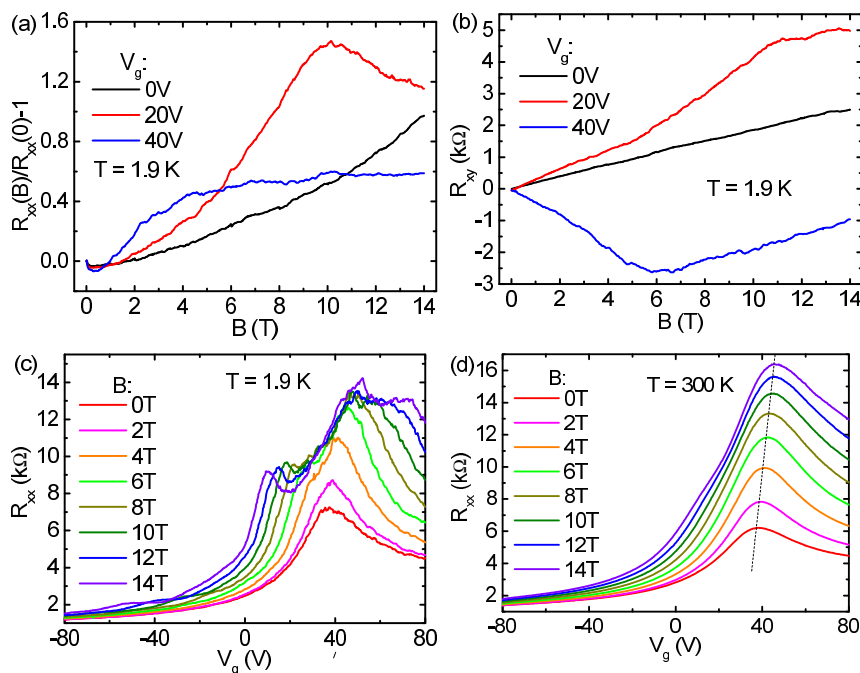

Figure 4 | Magnetotransport in two-stacked graphene monolayers. (a) The magnetoresistance described as $R_{xx}(B)/R_{xx}(0)-1$ at $V_g = 0$ V, 20 V and 40 V at 1.9 K. (b) Hall resistance at $V_g = 0$ V, 20 V and 40 V at 1.9 K. (c, d) Longitudinal resistance R_{xx} as a function of the back-gate voltage at various magnetic fields at (c) 1.9 K, and (d) 300 K.

www.nature.com/**scientificreports**

the carrier density by gate voltage decreases with increasing magnetic field. The weakening tunability of the carrier density by gate voltage may be due to the decoupling between the two-stacked graphene monolayers under high magnetic field, as graphene is of diamagnetic nature.

In summary, we develop a new method of mass production of two-stacked graphene monolayers with a clean interface. We perform Raman and electronic transport measurements on our two-stacked graphene monolayers. The Raman spectrum similar to that of a monolayer graphene shows that the two graphene monolayers remain independent. The electronic transport properties of the two-stacked graphene monolayers are quite different from mono-layer and bilayer graphene. We observe the asymmetric resistance-gate voltage curves and the maxima of the resistance-gate voltage curves shift with the magnetic field. The SdH oscillations indicate the 8-folded degeneracy of each Landau level.

Methods

Monolayer graphene was grown on Cu foils in a tube furnace by CVD method. PMMA thin film was used to carry the graphene after etching Cu. Another Cu/graphene was used to stack with the graphene/PMMA. The graphene/graphene/PMMA thin film was then patterned into microstamps using PMMA as resist and EBL technique. The graphene/graphene/PMMA film was then suspended after etching the Cu. The graphene/graphene/PMMA microstamps were transferred and printed onto SiO$_2$/Si substrate using a micromanipulator under an optical micro-scope. The two-stacked graphene monolayers were then fabricated into Hall bar geometry using EBL and oxygen plasmas etching. Metal electrodes were fabricated to contact with the graphene Hall bar by another round of EBL and metal deposition using electron-beam evaporation. The devices were placed in an Oxford cryostat instrument with temperature ranging from 300 K to 1.5 K and magnetic field up to 14 T. The electrical signals were measured using low frequency lock-in techniques.

1. Li, X. *et al.* Large-Area Synthesis of High-Quality and Uniform Graphene Films on Copper Foils. *Science* **324**, 1312–1314 (2009).
2. Suk, J. W. *et al.* Transfer of CVD-Grown Monolayer Graphene onto Arbitrary Substrates. *ACS Nano* **5**, 6916–6924 (2011).
3. Britnell, L. *et al.* Field-Effect Tunneling Transistor Based on Vertical Graphene Heterostructures. *Science* **335**, 947–950 (2012).
4. Dean, C. R. *et al.* Boron Nitride Substrates for High-Quality Graphene Electronics. *Nat. Nano.* **5**, 722–726 (2010).
5. Yang, H. *et al.* Graphene Barristor, a Triode Device with a Gate-Controlled Schottky Barrier. *Science* **336**, 1140–1143 (2012).
6. Bertolazzi, S., Krasnozhon, D. & Kis, A. Nonvolatile Memory Cells Based on MoS$_2$/Graphene Heterostructures. *ACS Nano* **7**, 3246–3252 (2013).
7. Gorbachev, R. V. *et al.* Strong Coulomb Drag and Broken Symmetry in Double-Layer Graphene. *Nat. Phys.* **8**, 896–901 (2012).
8. Kim, S., Jo, I., Nah, J., Yao, Z., Banerjee, S. K. & Tutuc, E. Coulomb Drag of Massless Fermions in Graphene. *Phys. Rev. B* **83**, 161401 (2011).
9. Kim, S. & Tutuc, E. Coulomb Drag and Magnetotransport in Graphene Double Layers. *Solid State Commun.* **152**, 1283–1288 (2012).
10. Lozovik, Y. E., Ogarkov, S. L. & Sokolik, A. A. Condensation of Electron-Hole Pairs in a Two-Layer Graphene System: Correlation Effects. *Phys. Rev. B* **86**, 045429 (2012).
11. Basu, D., Register, L. F., Reddy, D., MacDonald, A. H. & Banerjee, S. K. Tight-Binding Study of Electron-Hole Pair Condensation in Graphene Bilayers: Gate Control and System-Parameter Dependence. *Phys. Rev. B* **82**, 075409 (2010).
12. Landgraf, W., Shallcross, S., Türschmann, K., Weckbecker, D. & Pankratov, O. Electronic Structure of Twisted Graphene Flakes. *Phys. Rev. B* **87**, 075433 (2013).
13. Chen, J. J. *et al.* Layer-by-Layer Assembly of Vertically Conducting Graphene Devices. *Nat. Commun.* **4**, 1921 (2013).
14. Meng, J., Chen, J. J., Yan, Y., Yu, D. P. & Liao, Z. M. Vertical Graphene Spin Valve with Ohmic Contacts. *Nanoscale* **5**, 8894 (2013).
15. Brihuega, I. *et al.* Unraveling the Intrinsic and Robust Nature of van Hove Singularities in Twisted Bilayer Graphene by Scanning Tunneling Microscopy and Theoretical Analysis. *Phys. Rev. Lett.* **109**, 196802 (2012).
16. Reina, A. *et al.* Large Area, Few-Layer Graphene Films on Arbitrary Substrates by Chemical Vapor Deposition. *Nano Lett.* **9**, 30–35 (2008).
17. Schmidt, H., Lüdtke, T., Barthold, P. & Haug, R. J. Mobilities and Scattering Times in Decoupled Graphene Monolayers. *Phys. Rev. B* **81**, 121403 (2010).
18. Sanchez-Yamagishi, J. D., Taychatanapat, T., Watanabe, K., Taniguchi, T., Yacoby, A. & Jarillo-Herrero, P. Quantum Hall Effect, Screening, and Layer-Polarized Insulating States in Twisted Bilayer Graphene. *Phys. Rev. Lett.* **108**, 076601 (2012).
19. Chae, D.-H., Zhang, D., Huang, X. & von Klitzing, K. Electronic Transport in Two Stacked Graphene Monolayers. *Nano Lett.* **12**, 3905–3908 (2012).
20. Bie, Y.-Q. *et al.* Site-Specific Transfer-Printing of Individual Graphene Microscale Patterns to Arbitrary Surfaces. *Adv. Mater.* **23**, 3938–3943 (2011).
21. Parish, M. M. & Littlewood, P. B. Classical Magnetotransport of Inhomogeneous Conductors. *Phys. Rev. B* **72**, 094417 (2005).
22. Poumirol, J.-M., Escoffier, W., Kumar, A., Raquet, B. & Goiran, M. Impact of Disorder on the $v = 0$ Quantum Hall Plateau in Graphene. *Phys. Rev. B* **82**, 121401 (2010).

Acknowledgments

This work was supported by MOST (Nos. 2013CB934600, 2013CB932602), NSFC (Nos. 11274014, 11234001), and the Program for New Century Excellent Talents in University of China (No. NCET-12-0002).

Author contributions

Z.M.L. conceived and designed the study. J.J.C. performed the experiments. J.M. fabricated the graphene microstamps. D.P.Y. gave scientific advice. J.J.C. and Z.M.L. wrote the manuscript. All authors contributed to discussion and reviewed the manuscript.

Additional information

Competing financial interests: The authors declare no competing financial interests.

How to cite this article: Chen, J.-J., Meng, J., Yu, D.-P. & Liao, Z.-M. Fabrication and Electrical Properties of Stacked Graphene Monolayers. *Sci. Rep.* **4**, 5065; DOI:10.1038/srep05065 (2014).

This work is licensed under a Creative Commons Attribution-NonCommercial-ShareAlike 3.0 Unported License. The images in this article are included in the article's Creative Commons license, unless indicated otherwise in the image credit; if the image is not included under the Creative Commons license, users will need to obtain permission from the license holder in order to reproduce the image. To view a copy of this license, visit http://creativecommons.org/licenses/by-nc-sa/3.0/

SCIENTIFIC **REPORTS** | 4 : 5065 | DOI: 10.1038/srep05065   4